# Journal of Materials Chemistry B

Accepted Manuscript






ROYAL SOCIETY OF CHEMISTRY

www.rsc.org/materialsB

# Stimulation of wound healing by PU/hydrogel composites containing fibroblast growth factor-2

Yiu-Jiuan Lin[1], Ga-Hwa Lee[2], Chih-Wei Chou[3], Yi-Peng Chen[4], Te-Hsing Wu[5], Hong-Ru Lin[2,*]

[1]Department of Nursing
Chung Hwa University of Medical Technology, Tainan 717, Taiwan
[2]Department of Chemical and Materials Engineering
Southern Taiwan University of Science and Technology, Tainan 710, Taiwan
[3]Department of Cosmeceutics, College of Pharmacy
China Medical University, Taichung 404, Taiwan
[4]Department of Biotechnology
Southern Taiwan University of Science and Technology, Tainan 710, Taiwan
[5]Institute of Nuclear Energy Research, Taoyuan 32546, Taiwan

*Corresponding author: Hong-Ru Lin, Professor, Department of Chemical and Materials Engineering, Southern Taiwan University of Science and Technology, Tainan 710, Taiwan
Tel: +886-6-253-3131; Fax: +886-6-242-5741; E-mail address: hrlin@mail.stust.edu.tw (H. R. Lin)

**Abstract**

In this study, Polyurethane (PU)/hydrogel composites were fabricated for wound healing applications. Hydrogel is a copolymer of thermosensitive N-isopropyl acrylamide (NIPAAm) and acrylic acid (AAc). γ-ray irradiation was employed to simultaneously copolymerize NIPAAm with AAc and graft hydrogel onto porous PU. Fibroblast growth factor-2 (FGF-2) was incorporated into the composite to facilitate wound healing. The physical properties of composites were characterized, the *in vitro* release of FGF-2 was examined, and *in vivo* tests were conducted. The results indicate that thermosensitive hydrogel can absorb most of the wound exudates since its high water uptake ability. Due to its thermosensitive property, PU/hydrogel composite is easier to strip off than that of commercial wound dressing, which prevents additional

injury to the wound when replacing the wound dressing. *In vivo* results show that the PU/hydrogel composite incorporating FGF-2 could accelerate wound healing and reduce scar formation.

*Keywords*: Polyurethane (PU); N-isopropyl acrylamide (NIPAAm); Acrylic acid (AAc); Hydrogel; Fibroblast growth factor-2(FGF-2); $\gamma$ -ray; Wound healing; Wound dressing

## 1. Introduction

Large area burns or wounds have to be cured in the hospital, and some severe cases have even caused death [1, 2]. Therefore, in order to provide a useful method for wound healing, an alternative needs to be developed for the treatment of skin burns, skin ulcers, deep wounds and other trauma [3-5]. In the early stage of wound healing, several critical points must be considered, such as infection that could lead to inflammation, dryness or wetness of the wound's surface, permeability, and peeling [6]. All of these factors can potentially affect the wound healing process. When the skin tissues are damaged in the early stage, inflammation may occur, which would cause the healing time to be longer. Therefore, if bacterial infections can be suppressed in the early stage of treatment, bacterial invasion can be prevented, which would be beneficial for further wound treatment and healing. In addition, caring for the surface of the wound is also very important. In 1960, some researchers suggested that keeping the wound surface moist might help to speed up the healing process [1]. Moreover, having better permeability might prevent excessively wet or dry wounds to further promote wound healing. Another very important feature during wound healing involves whether the dressing is easy to remove or not. When the wound is almost healed, the dressing must be removed from the skin's surface. At that moment, the wound has just generated a lot of fresh granulation tissues, which are very fragile. If these granulation tissues become attached to the dressing, then removing the dressing might remove them at the same time, causing additional injury and more pain to the patient. Therefore, if the wound dressing is easy to strip off, a second injury and additional pain can be prevented. Based on the above reasons, an ideal wound dressing would have the following characteristics: 1. encouraging vapor exchange; 2.high absorption; 3. preventing bacteria from entering and causing infection; 4. antibacterial in nature; 5. promoting wound healing; and 6. easily removed [3, 7].

Wound healing is a very complex process, involving a series of processes caused by biologically active substances, including inflammation, immune cells migration, proliferation of fibroblasts, angiogenesis, collagen deposition, and scar formation [8]. Throughout these processes, many different cytokines play decisive roles in wound

healing. Among them, FGF-2 has been considered in a number of wound healing studies because FGF-2 is not only one of the most important substances in wound healing, but can also promote angiogenesis, which plays an important role in reproductive physiology [9, 10]. During the wound healing process, FGF-2 is used as an angiogenic precursor; afterwards, an angiogenesis series will be launched, which will first induce microvascular formation [11, 12]. In the meantime, it will regulate FGF-2 interstitial formation [13]. Finally, a scar will be formed to finish the wound healing process. Spyrou et al. [14] reported that FGF-2 can effectively delay scar contraction, making it considerably less visible. However, the application of FGF-2 in healing-impaired wound treatments has not always been successful *in vivo* due to its high diffusibility and very short half-life time *in vivo* to retain its biological activity [15, 16]. Therefore, an appropriate carrier to carry FGF-2 becomes essential in order to apply it in wound repair and tissue regeneration.

$\gamma$ -ray irradiation polymerization is based on Co-60 recession. The initiation of polymerization starts with γ-ray irradiation on a monomer, breaking C-H bonds of the monomer chain to generate radicals, and cationic or anionic ions. If moisture is contained in the irradiation, the ionic polymerization can be eliminated. When the C-H bonds are cleaved to generate radicals, the radicals will react with the C-H bond and the C = C bond or a monomer to generate a new radical. This process differs from polymerization at room temperature, which needs an initiator to break a double bond and then produces a chain reaction with the broken bonds for a long chain polymer [17]. Furthermore, γ-ray irradiation polymerization breaks not only a double bond but also a C-H bond. During polymerization, the polymer does not become a long chain but rather a polymer network structure. Thus, investigating the difference between polymerization at room temperature and γ-ray irradiation polymerization to form different polymer structures is very valuable.

Polyurethane (PU), due to its high biocompatibility, hydrophobic property, high mechanical strength, easy processing, and ability to modify surface functional features, is a very suitable material to be used in wound dressings [18, 19]. However, for the treatment of burns and wounds, such problems as improving the hydrophilicity, peeling and antibacterial properties of the substrate for the wound still remain. In this study, PU was used as the substrate. Thermosensitive N-isopropyl acrylamide (NIPAAm) and acrylic acid (AAc) were irradiated by γ-rays for hydrogel preparation. Hydrogel was grafted onto porous PU membrane to prepare the artificial PU/hydrogel composite wound dressings. To improve the mechanical properties of PU/hydrogel composite, clay was incorporated during the sample preparation. Clay is also used as antibacterial agent. Recently, inorganic minerals like clays and zeolites containing metals have achieved great significance compared to

conventional antibacterial agents. Thus, it is expected that PU/hydrogel composite has antibacterial property [20]. The PU/hydrogel composite was incorporated with FGF-2 to promote the wound healing process. The high permeability of the porous PU provides moderate mechanical strength while the thermosensitive hydrogel, due to its high water absorption ability, can absorb most of a wound's exudate. The lower critical solution temperature (LCST) of the PU/hydrogel composite can be regulated around the body temperature, making the dressing easy to remove so as not to cause additional damage to the wound when replacing the dressings. The swelling behavior, water vapor transmission rate, and antibacterial properties of the PU/hydrogel composites were investigated. The release profile of FGF-2 from PU/hydrogel composites was also conducted. In addition, *in vivo* testing using animal skin as the wound model was performed. The wound healing process was observed to assess the feasibility of the PU/hydrogel composites containing FGF-2 as wound dressings to accelerate wound healing.

## 2. Materials and Methods

### 2.1 Materials

Polyurethane (PU, Pellethane 2363-80A) was obtained from Lubrizol Advanced Materials, Inc., Cleveland, Ohio. Acrylic acid (AAc) was purchased from Merck (Germany) and N-isopropyl acrylamide (NIPAAm) from Wako (USA). Clay was supplied by a local company, Pai Kong Nanotechnology Ltd, Taiwan. Basic fibroblast growth factor-2 (FGF-2) was obtained from Cytolab, USA. All other chemicals and reagents used were of an analytical grade.

### 2.2 Preparation of porous PU membrane

An appropriate amount of Pellethane 2363 was added into dimethyl acetamide (DMAC) solvent formulated at 10 wt%, which was heated and stirred until completely dissolved. Then sodium chloride particles (<25 μm) with the weight 0.5 to 8 times the weight of polyurethane was added to the solution. The weight ratio between sodium chloride and polyurethane used to prepare samples for the wound healing test was 4 to 1. An appropriate amount of polyurethane solution containing sodium chloride was taken; after sonication, the solution was vacuumed to exhaust air bubbles and then poured into a Teflon container. It was then placed in an oven at 60 ~ 65℃ to dry. Then it was vacuumed until the solvent was completely drained. The polyurethane film (PU film) was taken out from the container and was immersed in 80℃ deionized water for 24 hours to remove the sodium chloride. The PU film free of sodium chloride was then dried in the oven at 60 ~ 65℃ again.

### 2.3 Preparation of PU/hydrogel composites

The PU film was placed in the homemade mold as shown in Figure 1. The aqueous solution containing 5 wt% clay was mixed with NIPAAm (98% molar ratio) and AAc (2% molar ratio) monomers. It was stirred until dissolved, and then the mixture was immediately injected into the space between two glass plates with a syringe. The gel membrane thickness was adjusted with a silicone spacer between the two glass plates. The whole fixture was received Co60 radiation, with an irradiation dose of 25 kGy to form hydrogel and to graft hydrogel into PU film simultaneously. The PU/ hydrogel composite was then rinsed with deionized water three times to remove unreacted monomers. Finally, they were dried at room temperature to make them free of moisture.

### 2.4 FT-IR Spectrum Analysis

The dried hydrogels were ground with potassium bromide in the ratio 1:99 in an agate mortar, and they were pressed to a disk. The Fourier transform infrared spectroscopy (FT-IR) spectra were obtained by using a Perkin Elmer infrared spectrometer (Spectrum One, USA).

### 2.5 Interior morphology observation of hydrogel

The prepared hydrogel was immersed in deionized water at 20℃ until equilibrium was attained. The swollen hydrogel was then frozen at -40℃ overnight prior to being subjected to lyophilization (FD-5N, EYELA, Japan). Specimen of the freeze-dried hydrogels was fractured carefully and its interior morphology was observed by scanning electron microscopy (SEM, S-3000N, Hitachi, Japan). Before conducting SEM observation, the specimen was fixed on aluminum stubs and coated with gold for 60 s.

### 2.6 Mechanical Tests

The PU/hydrogel composite was immersed in deionized water at 20℃ until equilibrium was attained. The compression measurements were performed on a swollen PU/hydrogel composite by using a universal material tester (AG-IS, Shimadzu, Japan) at a compression rate of 10 mm/min. The data were used to calculate the shear modulus ($G$) and cross-linking density ($\rho_x$) [21] using equations (1) and (2):

$$\tau = F/A = -G(\lambda - \lambda^{-2}), \quad (1)$$

$$\rho_x = G v_2^{-1/3}/RT, \quad (2)$$

where τ denotes the compression stress, $F$ the compression load, $A$ the cross-sectional area of the swollen hydrogels and $\lambda$ the compression strain ($L/L_o$). For low strains, a plot of the shear stress versus $-(\lambda - \lambda^{-2})$ would yield a straight line

whose slope is the shear modulus. $v_2$ denotes the volume ratio of the hydrogel at absolute temperature $T$ and $R$ is the gas constant. Three specimens were measured.

The tensile tests were performed on hydrogel or PU/hydrogel composite (both has dimension of 30 mm × 10 mm × 2 mm) by using a universal material tester (AG-IS, Shimadzu, Japan) at a rate of 4 mm/min. The data of tensile stress and strain were reported based on average of three measurements.

**2.7 Swelling and water content test**

The dried hydrogel or dried PU/hydrogel composite (each has a weight of 0.54 g and with a dimension of 0.8 cm x 0.8 cm x 0.2 cm) was placed in a 20 ml phosphate buffered saline (PBS) solution and deionized water at 25℃, respectively. It was blotted with filter paper and weighed at particular time intervals, until the weight remained unchanged. The swelling ratio was calculated by the following equation.

$$\text{Degree of swelling (w / w)} = (W_s - W_o) / W_o \quad (3)$$

($W_o$: weight of dried hydrogel; $W_s$: weight of the hydrogel after absorbing water)

The dried hydrogel or dried PU/hydrogel composite was placed in 20 ml of an aqueous PBS solution, until it fully swelled in the PBS. It was then blotted with filter paper and weighed. The water content was calculated according to the following equation.

$$\text{Water content (\%)} = (W_t - W_o) / W_t \times 100 \quad (4)$$

($W_o$: weight of the dried hydrogel; $W_t$: weight of the swollen hydrogel after reaching equilibrium)

The dried PU/hydrogel composite was placed into a PBS solution at 4℃ until fully swelling and then weighed. Then the swelling test was conducted with a rising temperature (4 to 50℃) in the PBS solution. The swelling ratio and water content of the thermo-sensitive PU/hydrogel composites were determined at a specific temperature according to the above procedure.

**2.8 Measurement of water vapor transmission rate**

The specimens (PU/hydrogel composites, PU and 3M waterproof breathable dressings (TegadermTM, 3M Health Care, Neuss, Germany)) were dried out; cut into pieces larger than internal diameter (6.20 mm) but smaller than external diameter (8.45 mm) of the cap; the original top of the cap was removed and the specimen was placed on top of the cap. The cap with the specimen was fastened to the measured cup. The measured cup filled with water was placed on the desiccator set at room temperature and 0% relative humidity for 30 min. Subsequently, the initial weight of the measured cup was weighted immediately. After that, the measured cup was moved to another desiccator under the conditions of 35℃ and 35% relative humidity.

After an equilibrium state was reached, cups were weighed every 1 h in the first 6 h, and then the weight was recorded at 8, 12, 16, 24 h, respectively.

The water vapor transmission rates (WVTR) of the specimen was calculated at a given time interval by the following method:

$$WVTR = (m/\triangle t) \cdot 24/A \quad (g/m^{-2}d^{-1}) \qquad (5)$$

where $m$ = mass of water loss over the specified time interval (g); $\triangle t$ = time interval (h); and $A$ = the effective transfer area ($m^2$). The WVTR values were averaged from three measurements.

**2.9 FGF-2 release studies**

The enzyme-linked immunosorbent assay (ELISA reader, Anthos 2001, Anthos Labtec Instruments, GmbH, Eugendorf, Austria) was used to measure the absorbance of formulations containing various concentrations of FGF-2 at 450 nm to obtain the standard curve. 5 mg of dried hydrogel and 5 mg of dried PU/hydrogel composites were placed in 1 ml PBS containing FGF-2 (with a concentration of 1 μg/ml) at 4℃, respectively, until fully swollen for 48 hr. The amount of FGF-2 loaded in each specimen was calculated as the difference between the initial and final concentrations in the surrounding solution, determined by ELISA at 450 nm. The changes in the concentration in the loading medium over time were recorded and the loading was considered to be finished when an equilibrium was reached (generally after 48 hr).

The swollen hydrogel and PU/hydrogel were then placed in 1 ml of PBS solution, respectively. After a desired period of time, certain amount of aliquot was withdrawn and the releasing amount of FGF-2 was analyzed by ELISA. The sample was placed in another bottle containing 1 ml of PBS, and then the absorbance was determined using ELISA until FGF-2 was no longer released. The drug release study was carried out at 25℃and 37℃, respectively.

**2.10 Antibacterial assessment**

The antibacterial test was conducted on aseptic bench. Firstly, the standard strains *Pseudomonas aeruginosa* and *Staphylococcus aureus* were dispersed to liquid medium, respectively, with temperature of the environment set as 37℃, pH value 7.4, and rotational speed 150 rpm, to culture and activate for 24 hours. Subsequently, 1 ml of medium containing bacteria liquid (with a bacteria concentration of $1x10^6$ CFU/ml) was taken and added to 10 ml of new liquid medium, and then a fixed amount of PU/hydrogel composite (with a diameter of 1 cm)was added and tested on preset time interval. The samples were removed after a specific time, and the UV absorbance (Lambda 25, Perkin Elmer, USA) was measured at the wavelength of 620

nm to observe the antimicrobial property of the PU/hydrogel composite.

### 2.11 Animal studies

Experimental animals were divided into five groups. Group 1 was non-treatment control. Group 2 was given only FGF-2. Group 3 was attached with PU/hydrogel only. Group 4 was attached with the PU/hydrogel composite with FGF-2. Group 5 was attached with commercial 3M dressings. All animal experiments were performed in compliance with guidelines approved by the Animal Use and Care Administrative Advisory Committee at the Southern Taiwan University of Science and Technology, Tainan, Taiwan.

First, the five groups of mice were anesthetized; their back hair was removed and the wound site was sterilized with alcohol. Full-thickness skin of 0.785 $cm^2$ was cut (a Wistar Rat for three wounds). The appropriate dressing material was placed on the wounds according to the groups. The bandage was fixed to the Wistar Rat's head and neck. Each rat was fed separately with an adequate supply of food and water. A photo was taken immediately after excision and then the wound area was determined. The wound area was measured from 0 to 10 days, and all of the measured data was compared with day 0. If the area is less than that of day 0, the wound is getting better. All mice were euthanized on days 0, 4, 10 and 20.

Wound closure (%) = $(A_d / A_o) \times 100$ (6)

($A_o$: initial wound area; $A_d$: wound area of d day)

In a specific time, after anesthesia of the Wistar Rat, the wound tissues from surrounding and subcutaneous skin were retrieved. The wound tissues were placed in a bottle containing 10% formalin for paraffin embedding and section. The thickness of the slice was 5 $\mu$ m. The slice was fixed on a slide coated with poly-L-lysine. After drying at 45℃, the samples were analyzed with Hematoxylin and eosin (H & E) and CD-71 staining. Afterwards, the mice were euthanized with an excess of carbon dioxide.

### 2.12 Statistical analysis

Results are given as means ± SD. Statistical analysis was performed using Student's t test. Statistical significance was set at $P < 0.05$.

## 3. Results and Discussion

### 3.1 Preparation of PU/hydrogel composite

In this study, a hydrogel copolymer composed of NIPAAm and AAc were formed by γ-rays irradiation. Hydrogel was then grafted onto porous PU membrane to prepare the artificial PU/hydrogel composite wound dressings.

Figure 2 shows the FTIR spectra of hydrogels including P(NIPAAm), PAA, and their copolymer P(NIPAAm-co-AAc). For P(NIPAAm) hydrogel, the main peak assignments are as follows: 3200-3400 $cm^{-1}$ (secondary amide N-H stretching), 2975 $cm^{-1}$ (-$CH_3$ asymmetric stretching), 1640 $cm^{-1}$ (secondary amide C=O stretching, aka amide I bond), and 1557 $cm^{-1}$ (secondary amide C=O stretching, aka amide II bond) [22]. For PAA hydrogel, the broad band at 3200-3500 $cm^{-1}$ is due to stretching vibration of –OH and the peak at 1720 $cm^{-1}$ is due to the presence of C=O stretching vibration [23]. All of these characteristic absorption peaks are all observed in P(NIPAAm-co-AAc) hydrogel prepared by $\gamma$ -ray irradiation excepting the peak of C=O stretching vibration from PAA is absent, which is due to the major component of this hydrogel copolymer is NIPAAm monomer (98% molar ratio). The spectrum of P(NIPAAm-co-AAc) hydrogel prepared at room temperature is also shown in Figure 2, which is very similar to the one prepared by $\gamma$ -ray irradiation, even though they form different polymer structures, i. e. long chain polymer vs. polymer network structure. The FTIR spectra provide evidence for the successful preparation of hydrogel copolymer P(NIPAAm-co-AAc) through $\gamma$ -ray irradiation.

The interior morphology of the lyophilized hydrogel and PU/hydrogel composite is observed with SEM and shown in Figure 3. All the hydrogels show interconnected pore structure with average void diameter of 188 μm. Therefore, it can absorb most of the fluid exudate and maintain certain water content in the wound bed. The pore structure allows the fibroblasts to divide and migrate within dressing. For PU/hydrogel composite, the PU membrane is grafted well to the hydrogel as shown in Figure 3 (b). The pore size of PU membrane is less than 25 μm. The pore size is large enough for water permeability.

For PU/hydrogel composite, the cross-link density increases from (1.3±0.5) $X10^6$ $mol/cm^3$ to (3.4±0.8) $X10^6$ $mol/cm^3$ as clay was incorporated to the specimen, which is about 2.6 times increase. According to equation 2, the larger the cross-link density, the greater the shear modulus, and renders a stiffer material. As shown in Figure 3 (c), clay is well dispersed and exfoliated in the polymer matrix and acts as a reinforcement agent, therefore, improving the mechanical property [24]. In addition, both tensile strength and strain of PU/hydrogel composite (326 ±24 KPa and 180.0 ±2.9%) are significant higher than those of hydrogel (5±1 KPa and 39.8±15.7% ). These data indicate PU layer provides the mechanical rigidity of the dressing, and it can prevent movement of the dressing during the wound healing. Thus, the bilaminar wound dressing prepared in this study is durable and allows for easy handling without tearing. Any disruption of the fragile wound surface can therefore be prevented.

### 3.2 Swelling and water content of PU/hydrogel composite

The dried hydrogel and PU/hydrogel composite (with dimensions of 0.8 cm x 0.8 cm x 0.2 cm for both specimens) were each placed in a PBS solution and deionized water, and swelling behavior was observed. Figure 4 shows the swelling curves of the hydrogel and PU/hydrogel composite at 25℃ and 37℃, respectively. The swelling behaviors of hydrogel and the PU/hydrogel composite were found to be different under different circumstances. The swelling ratio at 25℃ is higher than that at 37℃, due to NIPAAm's hydrophobic property at temperatures higher than its LCST (32℃). Therefore, raising the temperature reduces swelling and water content. Furthermore, the hydrogel and PU/hydrogel composite were observed to have a lower degree of swelling in the PBS than in the deionized water. We reasoned that AAc hydrogel is an ionic colloidal with large ion concentration, so in the PBS, ionic interactions between AAc hydrogel and PBS may occur, thus reducing the degree of swelling. Whether in the PBS or in deionized water, PU/hydrogel composite has a lower degree of swelling compared to hydrogel, which is due to the elastic force generated by PU film. Furthermore, PU has hydrophobic surface, thereby reducing the degree of swelling for composites. The swelling of the hydrogel is affected by the osmotic pressure inside and outside the hydrogel, as well as the same-charge-ion repulsive force. In this experiment, the ion force dominates the swelling behavior; therefore, in the PBS and deionized water, there is a balanced swelling behavior because the ionic concentration inside and outside the gel reaches equilibrium. According to the obtained results, ionic hydrogel is sensitive to a strong ionic environment, which is an important reference for composite wound dressing applications.

Table 1 lists the swelling ratio and water content of the hydrogel and PU/hydrogel composite in the PBS and deionized water after reaching equilibrium. The hydrogel and PU/hydrogel composite swelling at 25℃ have higher values than at 37℃, due to the NIPAAm in hydrogel, which is temperature sensitive. When the temperature increases, the hydrophobic phenomenon appears. The equilibrium water content of the PU/hydrogel composite at 37℃ reached 72% when immersed in the PBS, so its ability to absorb body exudates makes it very suitable as an artificial dressing. Furthermore, the degree of swelling of PU/hydrogel composite at 37℃ immersed in PBS is about 2.5 (w/w). Such a low value can cause extreme shrinkage of the PU/hydrogel composites and form skin to slow down the release of the FGF-2 in the PU/hydrogel composite. This is beneficial for sustained release of active ingredient in the wound healing.

Figure 5 shows the swelling ratio and water content of the PU/hydrogel composite with variation of temperatures. These properties were found to vary significantly with respect to temperature changes. As the temperature increases, the

PU/hydrogel composite slowly becomes hydrophobic and its degree of swelling and water content decrease. When temperature raised from 20 to 50℃, the swelling ratio of PU/hydrogel composite decreases about 468% and water content reduces about 36%. The abrupt change in these properties occurs at temperature slight higher than 30℃, which is close to the LCST of NIPAAm. NIPAAm has the characteristic of increasing hydrophobicity via temperature, due to the aggregation of NIPAAm's hydrophobic isopropyl groups [25]. The results indicate that the PU/hydrogel composite is temperature sensitive; this characteristic can be employed to control the FGF-2 release. On the other hand, the temperature of wound site is higher than the LCST of NIPAAm because of histamine being released from local inflammation [4]. When applied onto the surface of a wound site, the composite will absorb the exuded fluid and will be attached to the surface. The NIPAAm will become hydrophobic and fall off automatically once the wound site has healed. Therefore, it can prevent the second injury and additional pain when replacing the dressing.

**3.3 Water vapor permeability of PU/hydrogel composite**

In the water vapor permeability test, the PU, 3M waterproof and PU/hydrogel composite dressings were placed in the homemade water vapor permeability test device. Under 35℃ and 35% relative humidity, the WVTR was determined. The principle is when water enters the sample, it will be adsorbed on the surface of the sample, and then water molecules will diffuse out of the other side of the sample.

The WVTR of the PU/hydrogel composite (3340±164 $g/m^{-2}d^{-1}$) was found to be higher than that of the PU (2783±124 $g/m^{-2}d^{-1}$) and the commercial dressing (640± 102 $g/m^{-2}d^{-1}$), due to its larger hydrophilicity. Lamke et al. [26] reported that normal skin's WVTR is 204 ± 12 $g/m^2$/day, and the WVTR of skin with a first degree burn is 5138 ± 202 $g/m^2$/day. An ideal wound dressing would be able to control the rate of water loss from the wound, and prevent excessive exudates and dehydration. If there is no dehydration or excessive wound exudate, the WVTR is about 2000-3000 $g/m^2$/day [26]. With a hydrogel-containing layer (i.e. PU/hydrogel composite), the WVTR shows a greater trend, which is due to the higher hydrophilicity for adsorbing moisture. The structure of the commercial dressing is denser so water vapor cannot pass through it easily; thus, its WVTR value was lower than the PU/hydrogel composites. The WVTR value of the PU/hydrogel composite is close to the ideal range, which allows the wound to be maintained in a moist environment and can also absorb exudate effectively. In this environment, cells may migrate more easily as well in order to enhance the capacity of generating new skin.

### 3.4 FGF-2 release studies

Figure 6 shows the profile of FGF-2 release from the hydrogel and PU/hydrogel composite. An initial burst of release followed by a steadily sustained release was found. Whether at 25℃ or at 37℃, the release rate of the PU/hydrogel composite is faster than that of hydrogel, because PU is porous. Both the PU/hydrogel composite and hydrogel are found to release their FGF-2 slower at 37℃ than at 25℃. At 37℃, the shrinkage of NIPAAm makes a dense structure of the hydrogel, causing it to form a skin layer, which might delay the release of the FGF-2. At 25℃, the hydrogel is still in the water-swellable state, so the FGF-2 continues to release to the outside environment by mass transfer. As shown in the figure, about 55% of the FGF-2 is released on the first day from the PU/hydrogel composite at 37℃. The release of FGF-2 can last for at least seven days because the interactions between the negative charge of AAc (with $COO^-$) and positive charge of FGF-2 maintain its slow release. This prevents the fast release of FGF-2 due to its high diffusibility [15]. Therefore, the temperature sensitive feature of hydrogel can be used to control the release of the active ingredient, as well as to absorb the wound exudate and to keep the wound in a moist environment.

### 3.5 Antimicrobial property

Figure 7 shows the changes of optical density (OD) of *Pseudomonas aeruginosa* and *Staphylococcus aureus* cultured on the PU/hydrogel composite with the variation of time, respectively. The OD values increase with culture time until the growth reaches equilibrium. The OD values from the PU/hydrogel composite are lower than those from the control (bacteria liquid only). This result suggests that the PU/hydrogel composite has antimicrobial properties for these two bacteria, especially for *Pseudomonas aeruginosa*, since it can infect a wound. Therefore, the PU/hydrogel composite can serve as an excellent barrier, which provides an intact environment such that the wounded tissue can be prevented from being infected by external bacteria or virus while the wounded tissue is recovering to its original condition.

### 3.6 Observation of wound surface

In order to observe the wound area change, the images of the wound surface were captured and the area of the wound was determined to investigate the wound healing over time. Open wounds without any artificial dressings (groups of control and FGF-2 only) were found unable to keep the wound moist, thus forming scabs and reducing the rate of wound healing. Obvious scars were then generated (Figure 8). For PU/hydrogel and PU/hydrogel with FGF-2 groups, since the wound surface could

be kept in a moist state, the wound did not scab and scarring was less noticeable. For the commercial dressing group (3M waterproof breathable dressing), it is found that changing the dressing caused additional damage to the wound because it was not easy to remove. On the 20th day, the scar of the PU/hydrogel with FGF-2 group is found to have tightened significantly. The remaining four groups have obvious scars. In the control group and the group with FGF-2 only, pitted scars were observed because the wounds were open, which cannot keep them moist, resulting in scabs. When the scabs fell off, pitted scars had formed.

Figure 9 shows the percentage of wound closure versus healing time for these five groups. The healing capabilities for the groups of PU/hydrogel composite, commercial 3M and FGF-2 only were similar, while the PU/hydrogel containing FGF-2 showed to be better than the other four groups. FGF-2 has been proven to accelerate the wound healing process [16]. PU/hydrogel composites, commercial 3M and the PU/hydrogel containing FGF-2 all have the ability to keep the wound moist. However, the PU/hydrogel composite with FGF-2 is even better for wound healing because FGF-2 can promote the proliferation of fibroblasts. On the 10th day, the wound was 93% healed for the PU/hydrogel composite with FGF-2 group. With the other four groups, the wounds were less than 85% healed on the 10th day, showing a slower healing efficiency. Therefore, application of PU/hydrogel composite with FGF-2 is able to effectively interact with, protect and contract the wound, in a suitable moist healing environment.

**3.7 Histological analysis**

In order to observe the wound healing situation, the mice were euthanized and their skins were collected for histological analysis. Figure 10 shows tissue staining images for the wound contraction. The wounds were reduced with the increase of time for each group. It is speculated that the physical forces causing a wound to contract is initiated by adsorption of various protein molecules from the wound surface into the dressings [16]. The PU/hydrogel composite with FGF-2 exhibits the best results since it can provide a good healing environment that promotes cell migration. Adding FGF-2 can also promote wound healing, and therefore healing was faster than the rest of the four groups.

The H & E stained pathological sections of the wounds with different wound dressings on day 2 after the treatment are shown in Figure 11. The wound treated with PU/hydrogel with FGF-2 has a denser and larger epithelialization range than other groups. The commercial group showed loose epithelialization, while the control group did not produce epithelialization at all. This demonstrates that the wound healing of the PU/hydrogel with FGF-2 group is better than in the other

groups. Since hydrogel can keep the wound moist and contains large amounts of water, which can act as the extracellular matrix for the cells entering the hydrogel network structure, to increase epithelial cell migration and further promote wound healing and reduce scar formation [27]. Furthermore, granulation tissue (Fig. 11) and vascularization (Fig. 12) formation in FGF-2 incorporated PU/hydrogel-treated wounds progressed faster than in the control and commercial dressing. These results further confirm that the PU/hydrogel with FGF-2 has the best and fastest therapy effect of the groups tested.

## 4. Conclusions

PU/hydrogel composites were successfully fabricated for wound repair applications. Thermosensitive hydrogel can absorb most of the wound exudates due to its high water uptake ability. The prepared PU/hydrogel composite is easy to strip off and therefore can prevent additional injury to the wound when replacing the wound dressing. *In vivo* results demonstrate that the PU/hydrogel composite with FGF-2 could accelerate wound healing and reduce scar formation.

## 5. References

1. V. Yannas and J. F. Burke, J. Biomed. Mater. Res., 1980, 14, 65.
2. V. Yannas, J. F. Burke, et al., Science, 1982, 215, 174.
3. S. Y. Lin, K.S. Chen and R.C. Liang, Biomaterials, 2001, 22, 2999.
4. F. H. Lin, T. M. Chen, K. S. Chen, T. H. Wu and C. C. Chen, Mater. Chem. Phys., 2000, 64, 189.
5. R. A. Stile, W. R. Burghardt and K E. Healy, Macromolecules, 1999, 32, 7370.
6. R. A. Stile and K. E. Healy, Biomacromolecules, 2001, 2, 185.
7. A. B. Lugao and S. M. Malmonge, Nucl. Instrum. Meth. B, 1986, 185, 37.
8. M. B. Dreifke, A. A. Jayasuriya and A. C. Jayasuriya, Mat. Sci. Eng. C, 2015, 48, 651.
9. D. R. Knighton, G. D. Phillips and V. D. Fiegel, J. Trauma, 1990, 30, S134.
10. A. Baird, D. Schubert, N. Ling, and R. Guillemin, P. Natl. Acad. Sci. U.S.A., 1998, 5, 2324.
11. C. Richard, M. Roghani and D. Moscatelli, Biochem. Biophys. Res. Commun., 2000, 276, 399.
12. P. V. Murphy, N. Pitt, A. O'Brien, P. M. Enright, A. Dunne, S. J. Wilson, R. M. Duane and K. M. O'Boyle, Bioorg. Med. Chem. Lett., 2002, 12, 3287.
13. H. Yasui, A. Andoh, S. Bamba, O. Inatomi, H. Ishida and Y. Fujiyama, Digestion, 2004, 69, 34.
14. G. E. Spyrou and I. L. Naylor, Br. J. Plast. Surg., 2002, 55, 275.
15. K. Kawai, S. Suzuki, Y. Tabata, Y. Ikada and Y. Nishimura, Biomaterials, 2000, 21,

489.
16. K. Obara, M. Ishihara, T. Ishizuka, M. Fujita, Y. Ozeki, T. Maehara, Y. Saito, H. Yura, T. Matsui, H. Hattori, M. Kikuchi and A. Kurita, Biomaterials, 2003, 24, 3437.
17. L. Zhao, H. J. Gwon, Y. M. Lim, Y. C. Nho and S. Y. Kim, Radiat. Phys. Chem., 2015, 106, 404.
18. T. C. Wen, Y. J. Wang, T. T. Cheng and C. H. Yang, Polymer, 1999, 40, 3979.
19. T. C. Wen, S. S. Luo and C. H. Yang, Polymer, 2000, 41, 6755.
20. N. Ninan, M. Muthiah, N. A. B.Yahaya, I. K. Park, A. Elain, T. W. Wong, S. Thomas and Y. Grohens, Colloid. Surface B, 2014, 115, 244.
21. T. Jiang, W. I. A. Fattah and C. T. Laurencin, Biomaterials, 2006, 27, 4894.
22. Y. Cui, C. Tao, Y. Tian, Q. He and J. Li, Langmuir 2006, 22, 8205.
23. Y. J. Lin, F. C. Hsu, C. W. Chou, T. H. Wu, and H. R. Lin, J. Mater. Chem. B, 2014, 2, 8329.
24. Y. Zare and H. Garmabi, Appl. Clay Sci., 2015, 105-106, 66.
25. F. Liu and M. W. Urban, Prog. Polym. Sci., 2010, 35, 3.
26. L. O. Lamke, G. E. Nilsson and H. L. Reithner, Burns, 1977, 3, 159.
27. Z. Su, H. Ma, Z. Wu, H. Zeng, Z. Li, Y. Wang, G. Liu, B. Xu, Y. Lin, P. Zhang and X. Wei, Mat. Sci. Eng. C, 2014, 44, 440.

Table 1. The swelling ratio and water content of the hydrogel and PU/hydrogel composite in the PBS and deionized water after reaching equilibrium.

| Sample | Water content (%) | | Swelling ratio (w/w) | |
|---|---|---|---|---|
| | 25℃ | 37℃ | 25℃ | 37℃ |
| Hydrogel - W[a] | 98.60 | 98.06 | 70.89 | 50.75 |
| PU/Hydrogel - W | 95.51 | 92.97 | 21.34 | 13.24 |
| Hydrogel - P[b] | 94.02 | 86.57 | 14.55 | 6.46 |
| PU/Hydrogel - P | 89.51 | 71.59 | 8.57 | 2.52 |

[a]Hydrogel - W：Specimen immersed in water

[b]Hydrogel - P ：Specimen immersed in PBS

Figure captions

Figure 1. The homemade mold used to prepare hydrogel and PU/hydrogel composite.
Figure 2. FTIR spectra of P(NIPAAm), PAA, and their copolymer P(NIPAAm-co-AAc) prepared at room temperature and prepared by $\gamma$ -ray irradiation, respectively.
Figure 3. SEM observation of the interior morphology of the lyophilized (a) hydrogel, (b) PU/hydrogel composite, and (c) PU/hydrogel composite incorporated with clay.
Figure 4. The swelling profiles of hydrogel and PU/hydrogel composite at (a) 25℃and (b) 37℃, respectively.
Figure 5. The swelling ratio and water content of the PU/hydrogel composite with variation of temperature.
Figure 6. The release profile of FGF-2 from the hydrogel and PU/hydrogel composite at 25℃and 37℃.
Figure 7. The changes of optical density (OD) of Pseudomonas aeruginosa and Staphylococcus aureus cultured on PU/hydrogel composite with variation of time, respectively.
Figure 8. The image of wound surface healing over time in each group.
Figure 9. The percentage of wound closure versus healing time in each group ($p < 0.05$ as compared to control).
Figure 10. Histological examination of wound repair in each group. Arrows indicate edges of the epithelialization of each wound.
Figure 11. Histological examination of wound repair in each group on day 2 after initial wounding. The red arrow in the control group shows the location of epithelialization while the bracket in the other four groups indicate the range of epithelialization. The triangles show the granulation formation.
Figure. 12 Histological examination of wound repair in each group on day 2 after initial wounding. Arrows indicate the vascularization formation.

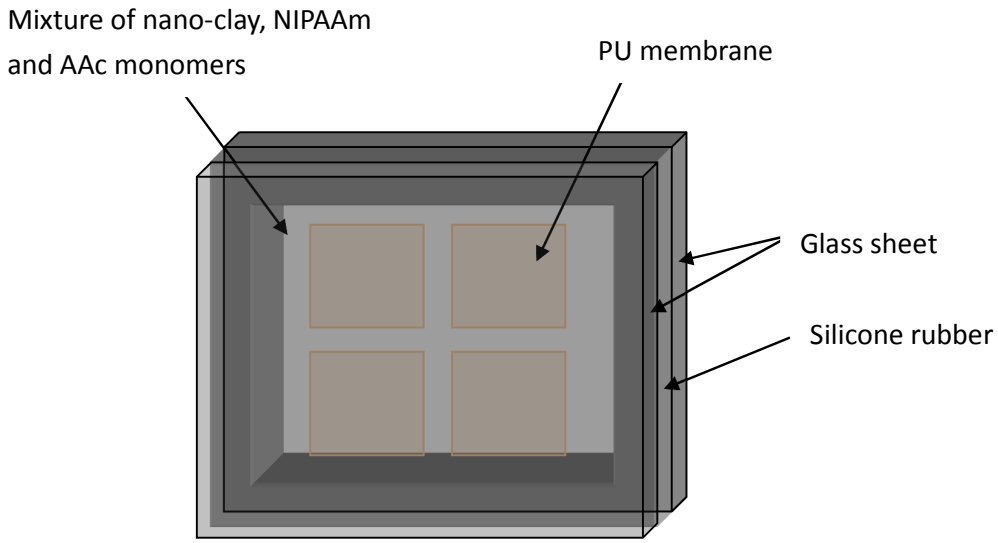


Figure 1. The homemade mold used to prepare hydrogel and PU/hydrogel composite.

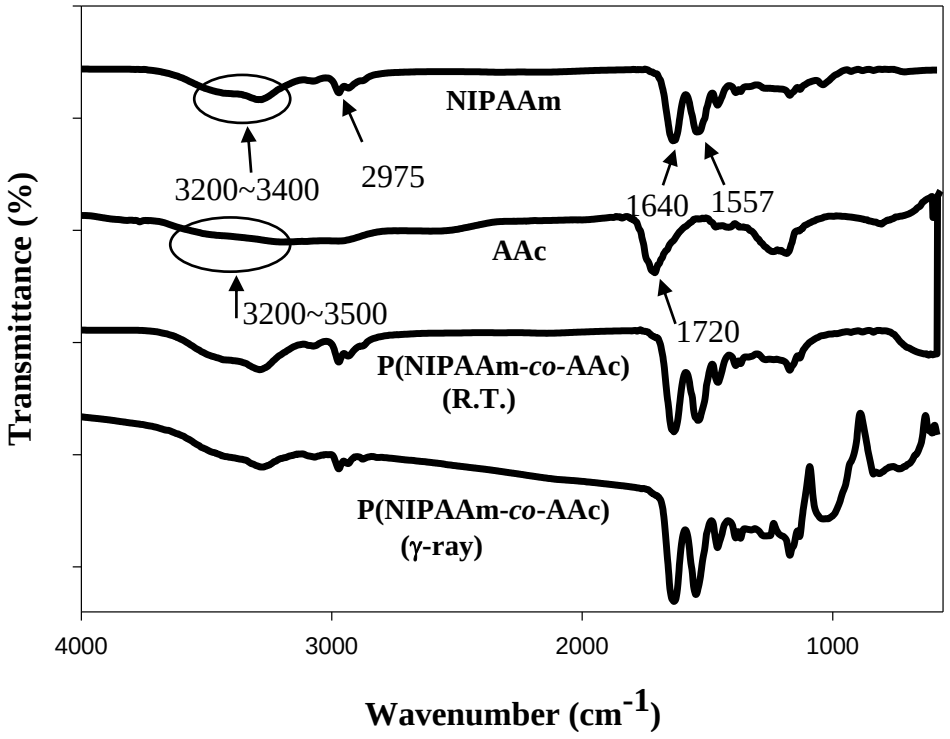


Figure 2. FTIR spectra of P(NIPAAm), PAA, and their copolymer P(NIPAAm-co-AAc) prepared at room temperature and prepared by γ-ray irradiation, respectively.

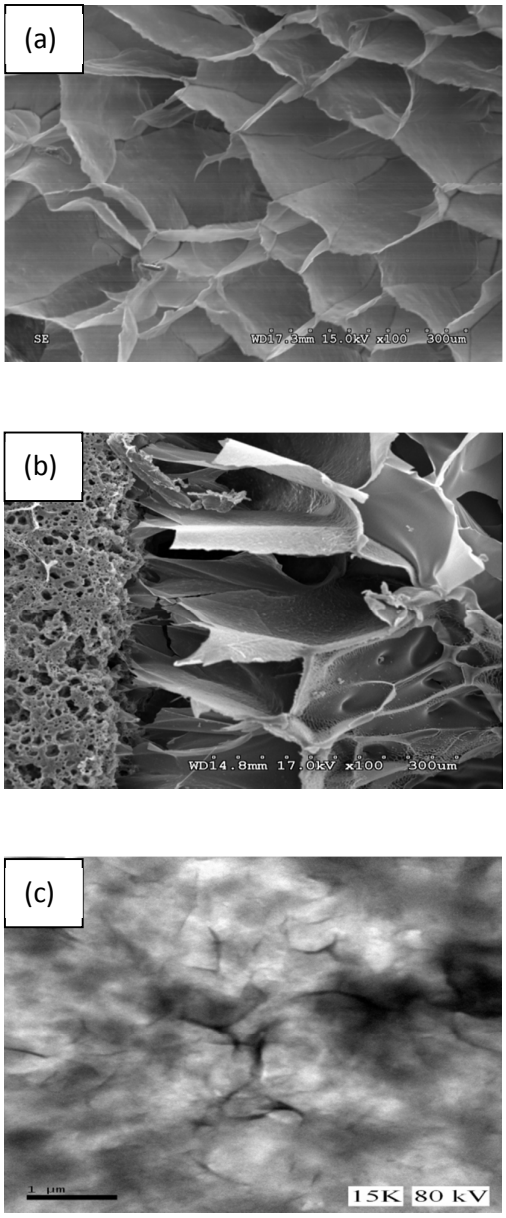


Figure 3. SEM observation of the interior morphology of the lyophilized (a) hydrogel, (b) PU/hydrogel composite, and (c) PU/hydrogel composite incorporated with clay.

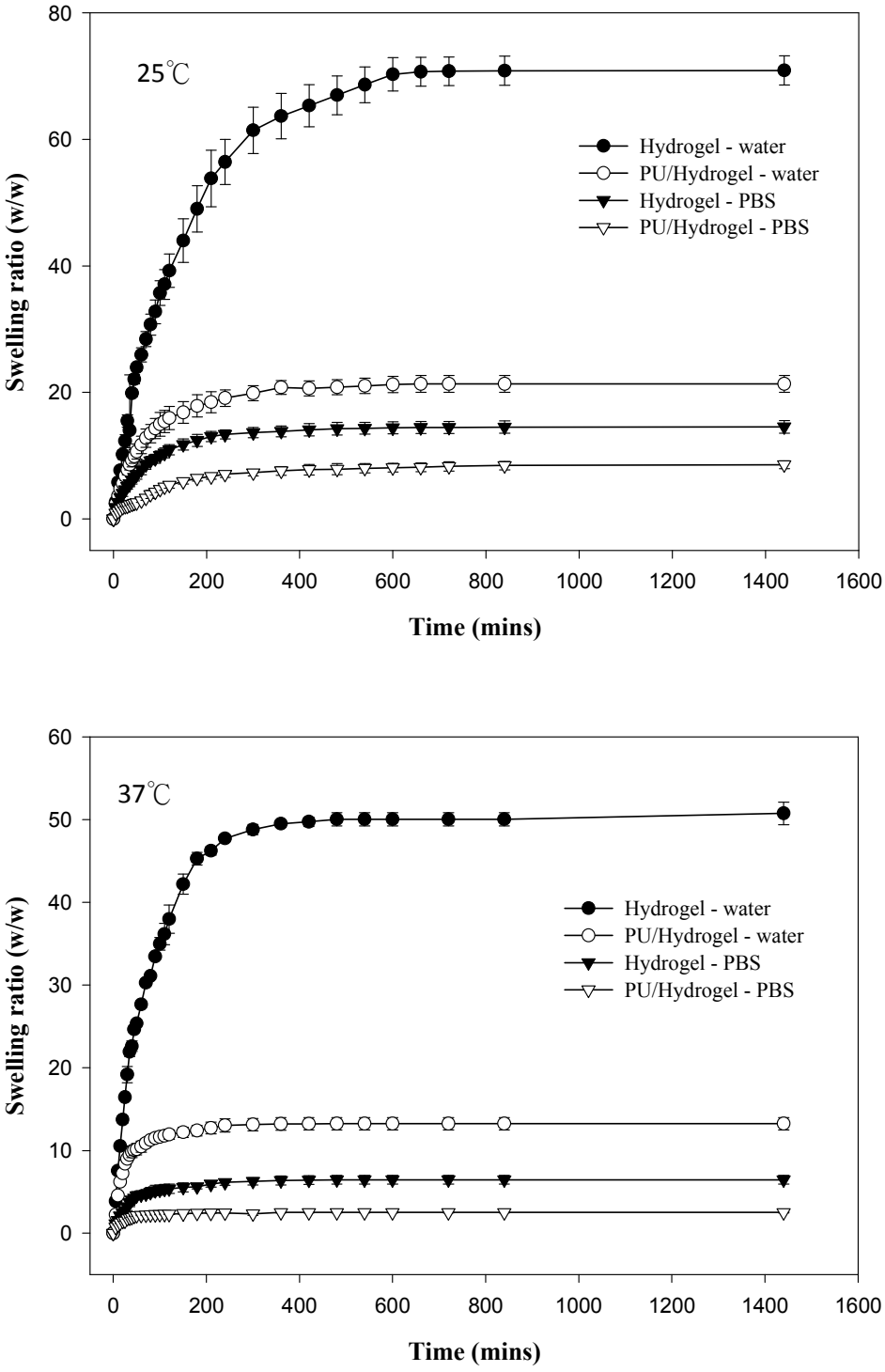


Figure 4. The swelling profiles of hydrogel and PU/hydrogel composite at (a) 25℃and (b) 37℃, respectively.

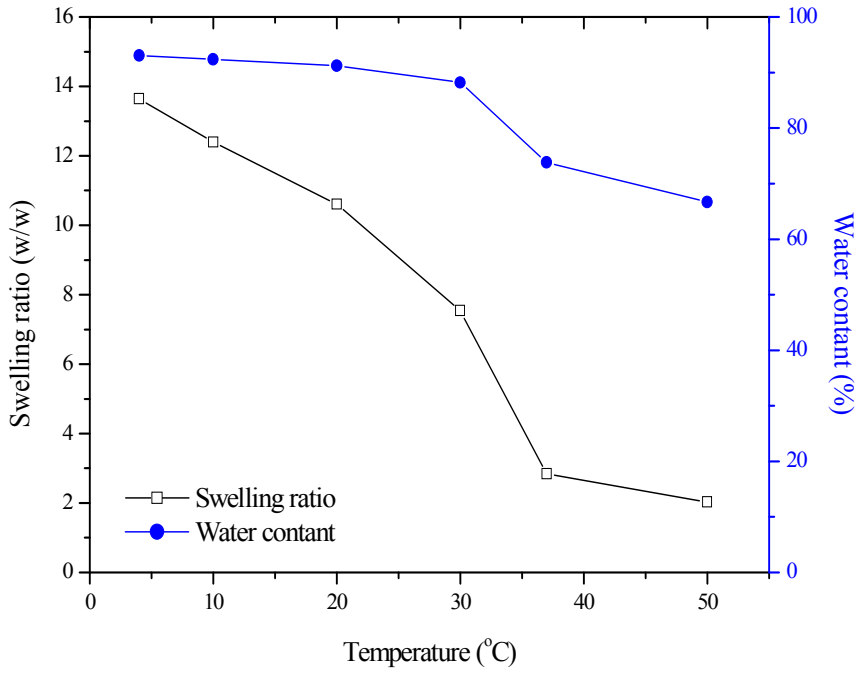


Figure 5. The swelling ratio and water content of the PU/hydrogel composite with variation of temperature.

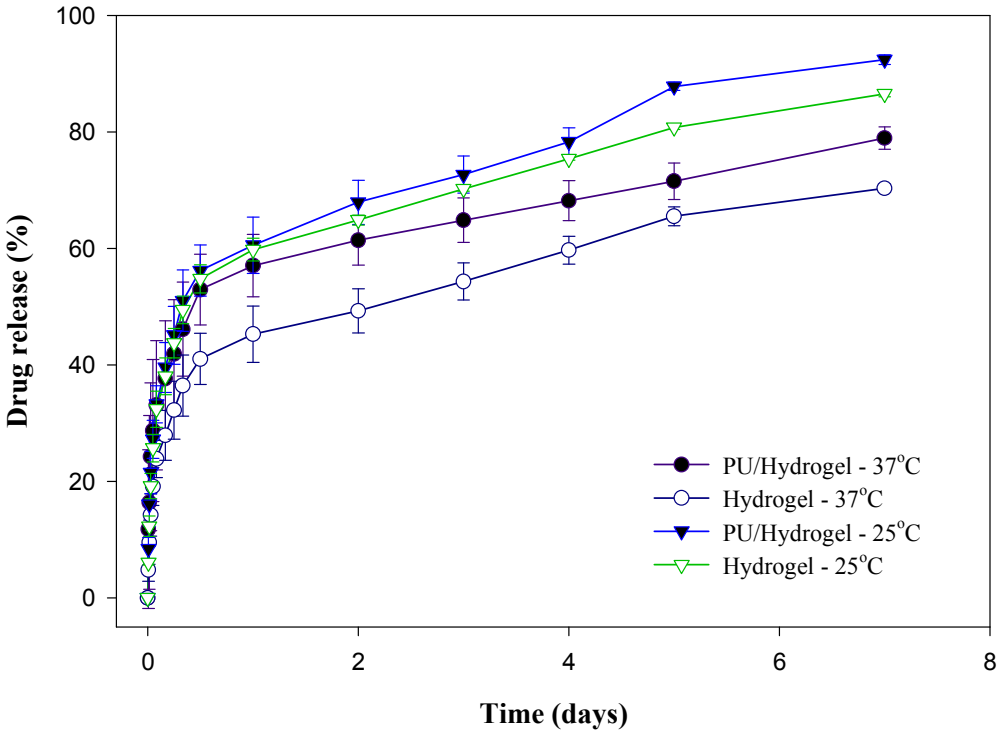


Figure 6. The release profile of FGF-2 from the hydrogel and PU/hydrogel composite at 25℃and 37℃.

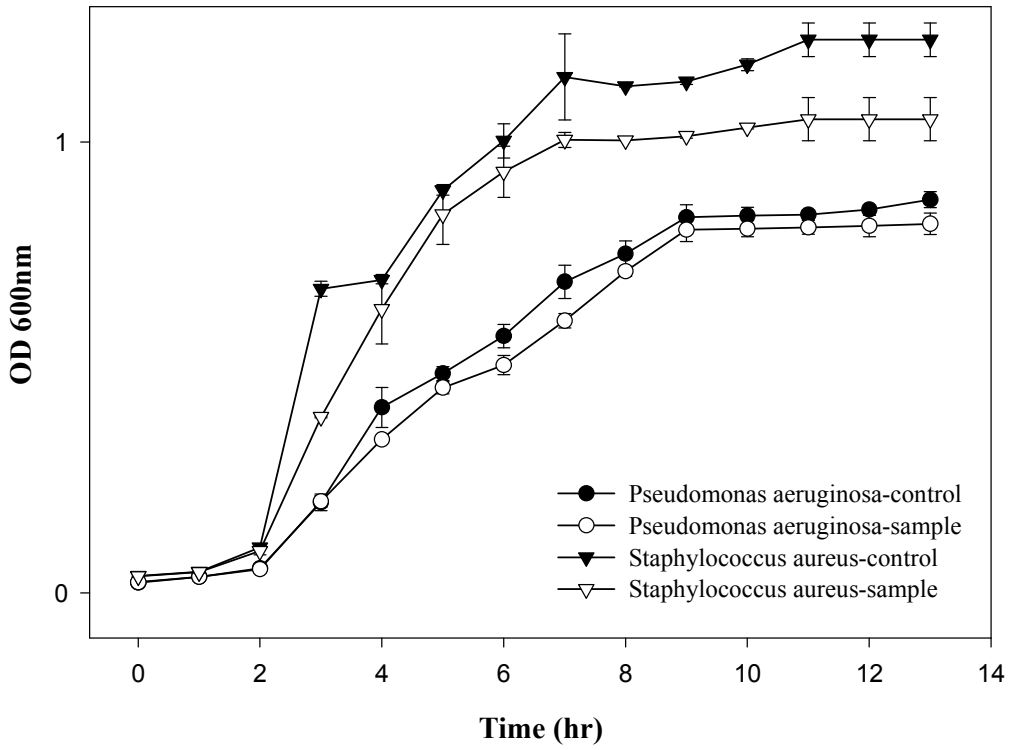


Figure 7. The changes of optical density (OD) of Pseudomonas aeruginosa and Staphylococcus aureus cultured on PU/hydrogel composite with variation of time, respectively.

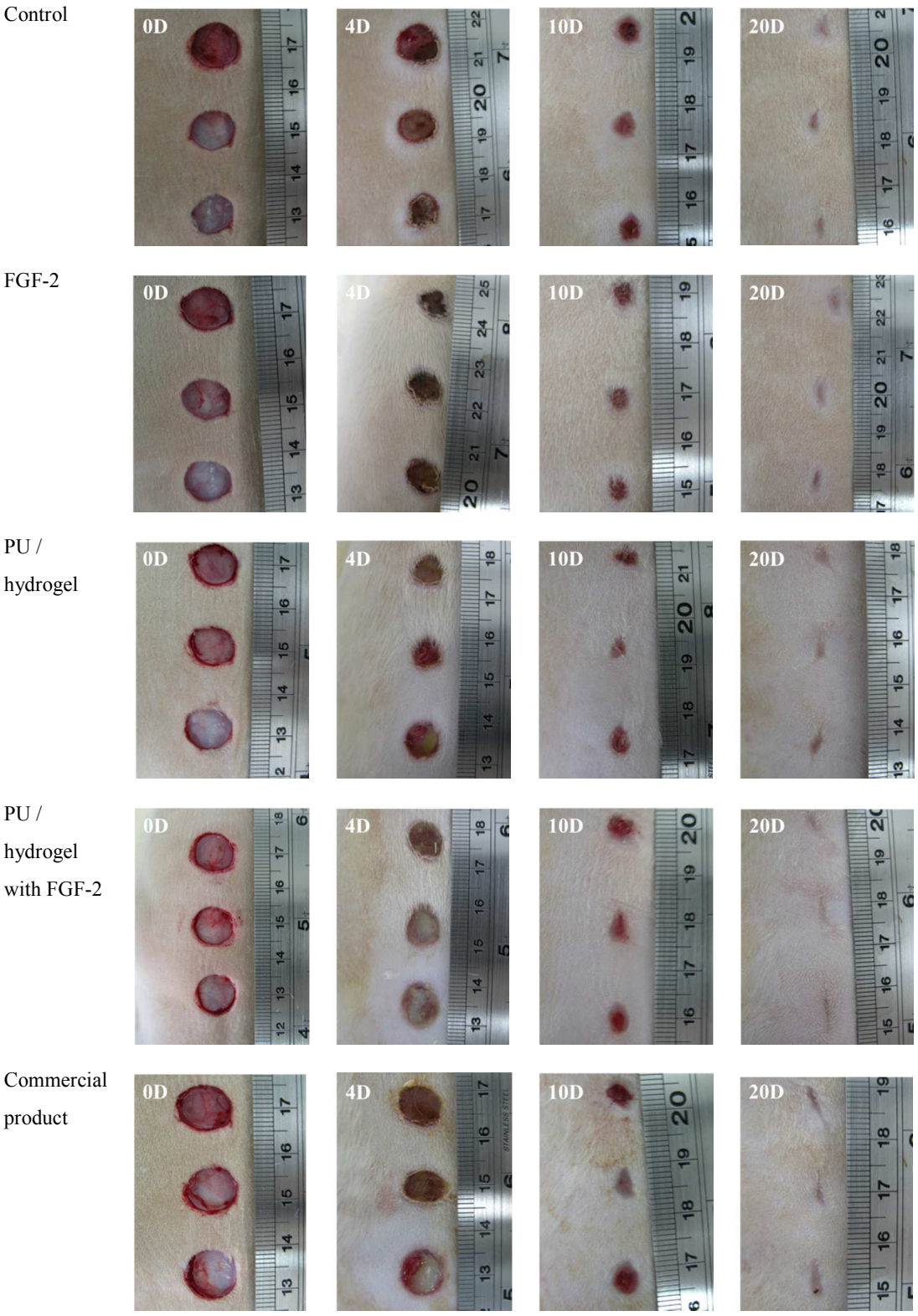


Figure 8. The image of wound surface healing over time in each group.

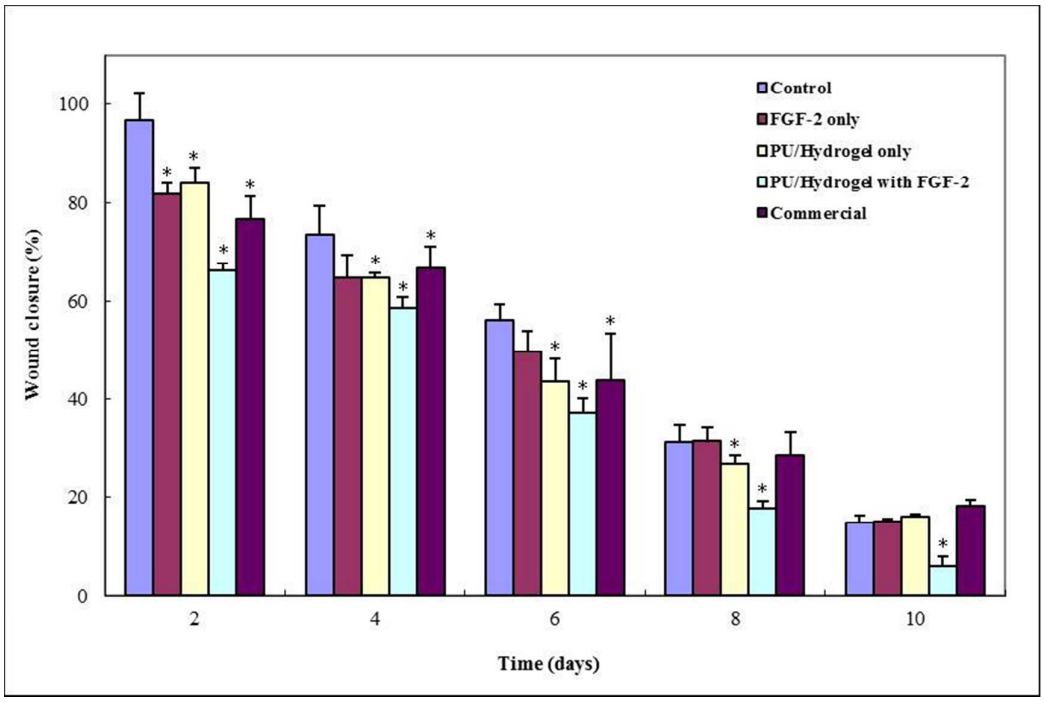


Figure 9. The percentage of wound closure versus healing time in each group ($p < 0.05$ as compared to control).

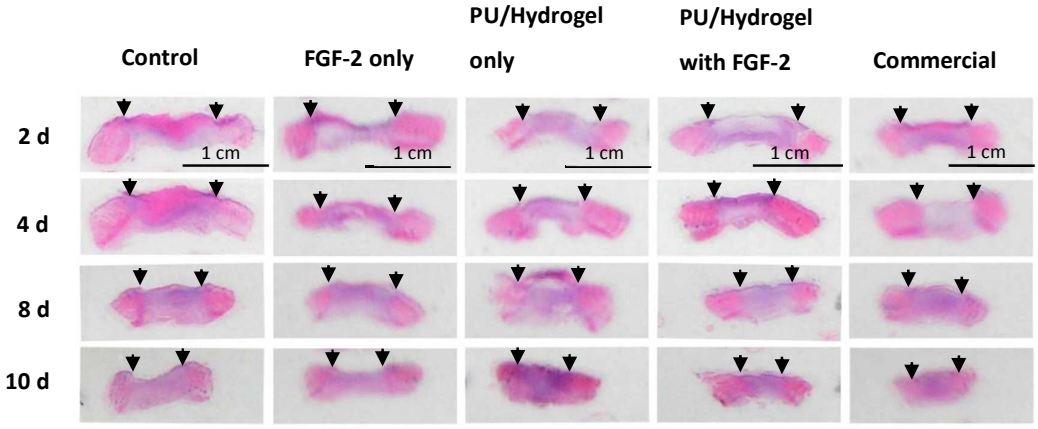


Figure 10. Histological examination of wound repair in each group. Arrows indicate edges of the epithelialization of each wound.

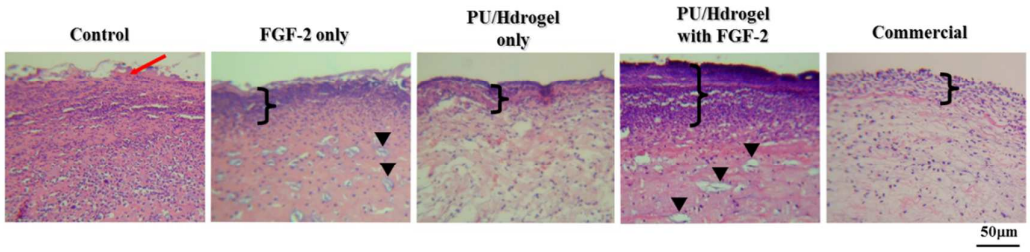


Figure 11. Histological examination of wound repair in each group on day 2 after initial wounding. The red arrow in the control group shows the location of epithelialization while the bracket in the other four groups indicates the range of epithelialization. The triangles show the granulation formation.

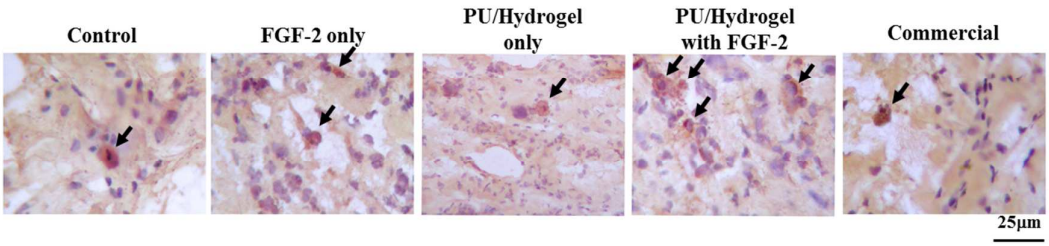


Figure. 12 Histological examination of wound repair in each group on day 2 after initial wounding. Arrows indicate the vascularization formation.

## Graphical and textual abstract

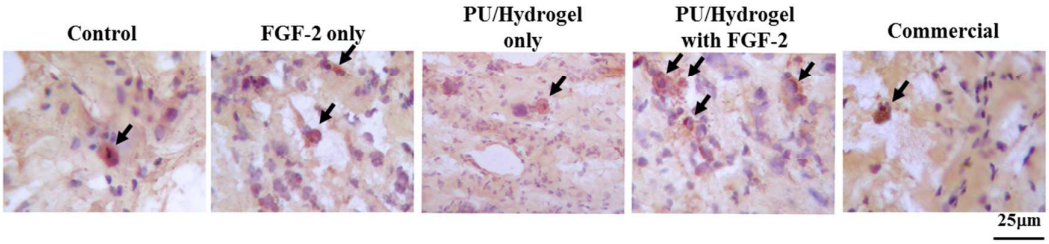


Histological examination of wound repair in each group on day 2 after initial wounding. Arrows indicate the vascularization formation.